


 Cite this: *RSC Adv.*, 2023, **13**, 30528

# Isolation, virtual screening, action mechanisms, chelation with zinc ions, and stability of ACE-inhibitory peptides from ginkgo seed globulin

 Wei Gao,<sup>a</sup> Min Liu <sup>\*b</sup> and Yu Wang<sup>\*b</sup>

Ginkgo seed has potential applications in the prevention and treatment of hypertension, but its application in food is limited. Thus, ginkgo seed globulin was hydrolyzed using dual enzymes (Alcalase and thermolysin). After gel column separation, reverse-phase high-performance liquid chromatographic purification, and ESI-MS/MS analysis, five oligopeptides containing fewer than 12 amino acid residues were obtained. Among them, the heptapeptide Glu-Ala-Ser-Pro-Lys-Pro-Val (EASPKPV) offered relatively high capacities to inhibit ACE (IC<sub>50</sub>: 87.66 μmol L<sup>-1</sup>) and bind with zinc ions (5.35 ± 0.32 mg g<sup>-1</sup>). Moreover, EASPKPV showed competitive inhibitory kinetics against ACE. Fourier-transform infrared spectroscopy analysis evidenced that the amino group and carboxyl group of EASPKPV could both provide binding sites for zinc ions. EASPKPV can restrain ACE in the following ways: (i) competitively linking with five key residues (Gln281, Ala354, Glu376, Lys511, and Tyr523) in the S1 and S2 pockets of ACE by short hydrogen bonds; (ii) binding to thirteen active residues of ACE *via* hydrophobic interactions; and (iii) binding with residue His383 or the zinc ion of zinc tetrahedral coordination. Additionally, simulated gastrointestinal digestion did not show any remarkable efficacy on the capacities of EASPKPV to restrain ACE and bind with zinc ions. These results indicate that ginkgo peptides may be used for antihypertension.

 Received 3rd August 2023  
 Accepted 3rd October 2023

DOI: 10.1039/d3ra05248f

[rsc.li/rsc-advances](http://rsc.li/rsc-advances)

## 1. Introduction

Currently, one in four deaths worldwide is due to high blood pressure. Preventing high blood pressure is a worldwide health problem.<sup>1</sup> Although the regulating mechanism of human blood pressure is complex, increasing clinical trials have demonstrated the important role of the ACE-Ang II-AT1R axis in regulating blood pressure, of which Angiotensin-I-Converting Enzyme (ACE) is found to play a crucial role in the elevation of blood pressure.<sup>2</sup> Thus, inhibition of ACE activity is one of the main action mechanisms of antihypertensive drugs to reduce blood pressure.<sup>3</sup> Over the past few decades, natural antihypertensive peptides, especially food-derived ACE-inhibitory peptides with *in vivo* antihypertensive effects, have received increasing attention because they are considered to be safer, more effective, and more economical than synthetic antihypertensive drugs.<sup>4</sup> Synthetic ACE-inhibitors such as captopril, enalapril, and ramipril (all heterocyclic compounds containing nitrogen) often have side effects for patients, including dizziness, headache, fatigue, cough, nausea, and diarrhea. In contrast, ACE-inhibitory peptides derived from dietary proteins

are safer, easier to absorb, and more readily available.<sup>3</sup> ACE is a zinc metalloproteinase. Its active center contains S1, S2, and S' pockets that consist of nine amino acid residues (Lys511, Tyr523, His353, Glu384, His513, Ala354, Glu162, Gln281, and Tyr520).<sup>5</sup> Peptides with strong binding power with one or more of the nine active sites in the ACE central pocket are found to be competitive inhibitors of ACE, whereas peptides that can affect the structure of ACE *via* binding with other residues outside the central pockets offer non-competitive inhibition activity toward ACE.<sup>6,7</sup> Moreover, ACE's zinc center, a zinc tetrahedral coordination that consists of a zinc ion linked with Glu411, His383, and His387 residues, catalyzes bradykinin hydrolysis.<sup>5</sup> Therefore, ACE can be inhibited by metal chelating agents or peptides of strong binding affinity with Glu411, His383, or His387 residue.<sup>8</sup> In recent decades, although peptides with inhibition effects on ACE have been obtained in animal protein, marine product, plant protein, and fish by-product hydrolysates,<sup>9,10</sup> investigation about the effect of peptides with zinc-chelating capacity on ACE activity and the action mechanism is little.

Now, the utilization of dietary peptides as ACE inhibitors is considered a practical way to prevent and improve hypertension.<sup>1</sup> However, substantial studies have found that food-derived peptides may lose their inhibition ability against ACE when they are subjected to different food processing conditions and the hydrolysis of gastrointestinal enzymes.<sup>8</sup> Heating and acidic or alkaline treatment can cleave chains of peptides.<sup>11</sup> Changes in pH value and ionic strength may change the

<sup>a</sup>School of Innovation & Entrepreneurship, Shanxi Agricultural University, Taigu, Shanxi 030801, China

<sup>b</sup>College of Food Science and Engineering, Shanxi Agricultural University, Taigu, Shanxi 030801, China. E-mail: liumin2023@yeah.net; sxtgw@126.com; Tel: +86-15011390837


electrochemical properties of peptides. Enzymes presenting in the stomach and intestines, such as pepsin, trypsin, and tripeptidase, can cleave peptides' chains, which can change the binding mode of peptides with ACE or zinc ions, resulting in a decrease in the ACE inhibitory effect of peptides.<sup>12,13</sup> Moreover, potential toxicity and sensitization may hinder the application of peptides in foods.<sup>2</sup> Therefore, except for the inhibition effect on ACE, the action mechanism, zinc chelating ability, and stability of antihypertensive peptides should be studied.

The ginkgo (*Ginkgo biloba* L.) tree is widely grown in China, New Zealand, Europe, the United States, India, and Argentina.<sup>14</sup> *Ginkgo biloba* is rich in bioactives such as biflavonoids, polyphenols, bilobalides, and alkyl coumarins.<sup>15</sup> The soft yellow seed of ginkgo (ginkgo kernel) is edible and used to treat kidney problems, coughs, asthma, neurological dysfunctions, and lung problems.<sup>16–18</sup> The protein content of ginkgo seed (14–23 g/100 g, dry weight basis) is nearly equal to that of soybean.<sup>19</sup> Albumin and globulin are the main protein fraction, accounting for approximately 75 g/100 g.<sup>20</sup> In China, the annual yield of ginkgo seed is around 6 kilotons, but the utilization of ginkgo seed is limited due to its potential toxicity or allergenicity.<sup>16</sup> Although antidiabetic, antihypertensive, and antibacterial peptides have been isolated from ginkgo protein isolates,<sup>21,22</sup> data about the ACE inhibition mechanisms, security, and physicochemical properties of peptides with zinc chelating capacity from ginkgo seed is limited. Our pre-experiments showed that the zinc-chelating ability and inhibition ability toward ACE of ginkgo seed globulin hydrolysates (GSGH) were  $5.16 \pm 0.17 \text{ mg g}^{-1}$  and  $67.67\% \pm 3.33\%$ , respectively, indicating that peptides possessing zinc-chelation and ACE inhibition capacities should be isolated from GSGH. Accordingly, the isolation, characterization, action mechanism, and zinc ion-chelating capacity of GSGH ACE inhibitory peptides were investigated in the present study. Additionally, we investigated the physicochemical characteristics and stability of GSGH ACE-inhibitory peptides.

## 2. Materials and methods

### 2.1. Materials and reagents

GuLing Apricot Garden (Taigu, China) donated fresh ginkgo seeds. Alcalase (USP, 1 : 30 000 U g<sup>-1</sup>), thermolysin (USP, 1 : 100 000 U g<sup>-1</sup>), trypsin (USP, 1 : 3000 U g<sup>-1</sup>), and pepsin (USP, 1 : 100 000 U g<sup>-1</sup>) were purchased from Yuanheng Keji Co. (Xi'an, China). ACE (0.25 U, derived from rabbit lung), *N*-hippuryl-L-histidyl-L-leucine (HHL), and captopril were purchased from Sigma (St. Louis, MO, USA). Anhydrous ethanol, zinc chloride, and other reagents were all analytical grades and purchased from Shuangyangguan Co. (Taigu, China).

### 2.2. Ginkgo seed globulin preparation

The shells of ginkgo seed were removed, and the soft kernel was dried at  $45 \pm 1 \text{ }^\circ\text{C}$  for 21 h.<sup>19</sup> The soft kernel was ground, and the obtained powder was placed into a triangular glass bottle. Petroleum ether (60–90 °C) was added at a ratio of 1 : 9 (g mL<sup>-1</sup>) to remove fat. The bottle was placed in an EZH-004C water bath

oscillator (Shangyu Instrument Factory, Zhuji, China) and gently stirred (65 rpm) at 30 °C for 180 min. Next, the mixture was filtered, and the residue on the filter paper was dried at 50 °C overnight. The dried residue was sieved using a sieve (ZJ-IIC, 100 mesh, Zhuji Sieve Factory, Zhuji, China) to get dried ginkgo seed kernel powder. In another triangular glass bottle, ten grams of defatted ginkgo seed powder and 350 mL of NaCl solution (0.25 mol L<sup>-1</sup>) were added. The bottle was shaken in a EZH-004C water bath oscillator at 185 rpm and  $40 \pm 1 \text{ }^\circ\text{C}$  for 2 h. After filtration, the filtrate was centrifuged at  $7300 \times g$  for 20 min. The supernatant was pooled and adjusted to pH 4.20  $\pm$  0.05 (the isoelectric point of ginkgo seed globulin),<sup>19</sup> and then placed at 4 °C for 80 min. Afterward, the solution was centrifuged again at  $7300 \times g$  and 5 °C for 25 min. The sediment was collected, re-dispersed in 10 mL dH<sub>2</sub>O, adjusted to pH 7.0, and then transferred into a membrane (cut-off mass of 3.5 kDa, Nengjing Membrane Co., Tianjin, China). After dialysis in dH<sub>2</sub>O at 4 °C for 1 d, the dialysis solutions were freeze-dried, and ginkgo seed globulin (GSG) was obtained.

### 2.3. Ginkgo seed globulin hydrolysates

Following the method of Ma *et al.* (2019),<sup>22</sup> in a triangular glass bottle, GSG (3 g), Alcalase (0.09 g), and 150 mL of phosphate buffer (0.1 mol L<sup>-1</sup>, pH 8.0) were added and mixed thoroughly. The bottle was placed in the EZH-004C water bath oscillator (50 °C) and shaken at a stirring rate of 225 rpm. After 90 min, thermolysin (0.09 g) was added, and the temperature was reduced to 37 °C. The proteolysis digestion was continued for another 90 min. Throughout the hydrolysis process, the reaction solution was maintained at pH  $8.0 \pm 0.1$  *via* the addition of NaOH (0.1 mol L<sup>-1</sup>) at 20 min intervals. The hydrolysis reaction was terminated by heating at 100 °C for 10 min. Then, the digestion solution was centrifuged at  $12\,700 \times g$  for 15 min, the supernatant was lyophilized, and ginkgo seed globulin hydrolysates (GSGH) were obtained. Moreover, hydrolysis degree measurement was done according to the method of Nielsen *et al.*<sup>23</sup>

### 2.4. Chromatographic purification

In the current study, ultrafiltration, gel chromatography, and reversed-phase high-performance liquid chromatography (RP-HPLC) were used in sequence to purify GSGH.<sup>24</sup> First, GSGH (2 mg mL<sup>-1</sup>) was pressed through an ultrafiltration membrane with an aperture of 0.22 μm (aqueous system, Jiteng Membrane Co., Tianjin, China). The percolate (2 mg mL<sup>-1</sup>) was loaded on a glass chromatographic column (16 × 1000 mm, Huwest, Xi'an, China), which was filled with Sephadex G-15 gel beforehand and equilibrated using dH<sub>2</sub>O. The gel chromatographic purification was conducted with an elution solution of dH<sub>2</sub>O (2.8 mL min<sup>-1</sup>) and a monitored wavelength of 220 nm. The gel chromatographic spectrum against elution time was drawn, and the subfractions (corresponding to adsorption peaks in the spectrum) were separately pooled, lyophilized, and used for determination of inhibition ability against ACE and chelating ability towards zinc ions.<sup>25</sup> Then, a LC-SPD-20C RP-HPLC system equipped with a SDOCI-4 chromatographic column (1.8 × 12.5 cm, 5 μm; Suprile, Hangzhou, China) was used for



further purification of the GSGH subfraction that showed the highest ability to inhibit ACE. Binary gradient elution was used at a rate of 1 mL min<sup>-1</sup> and 36 °C. The elution A was acetonitrile with an increasing concentration (0–35% in 15 min), and the elution B was 0.1% trifluoroacetic acid (v/v). The RP-HPLC spectrum was drawn, and the subfractions (corresponding to adsorption peaks in the spectrum) were separately pooled, lyophilized, and used for the determination of the abilities to inhibit ACE and chelate zinc ions.<sup>25,26</sup> The peptide sequence of the subfraction possessing the strongest inhibiting power for ACE was analyzed.

### 2.5. Restraining ability and kinetics on ACE

ACE-restraining ability was determined using the *N*-hippuryl-L-histidyl-L-leucine method.<sup>25</sup> Briefly, ACE solution (50 mU, in 0.1 mol L<sup>-1</sup> of borate buffer solution, pH 8.3) and GSGH peptide solution (1 mg mL<sup>-1</sup>, in 0.1 mol L<sup>-1</sup> of borate buffer solution, pH 8.3) were both pre-incubated at 37 °C beforehand. Then 100 μL of ACE solution, 100 μL of GSGH peptide solution, and 350 μL of *N*-hippuryl-L-histidyl-L-leucine (8 mmol L<sup>-1</sup>) were added into a glass test tube. The tube was placed in the EZH-004C water bath oscillator (37 °C) with a shaking rate of 125 rpm. One hour later, the reaction was terminated by the addition of HCl (0.1 mol L<sup>-1</sup>, 1.45 mL), and then 1.45 mL of ethyl acetate was added and thoroughly mixed. The mixture was centrifuged at 13 000 × *g* for 15 s, and the upper solution was transferred into another glass tube and heated in a blast drying oven (HKBS-2, Shanghai Hengke Instrument, Shanghai, China) at 125 °C. Ten minutes later, the glass tube was picked out, cooled to room temperature, and 1 mL of deionized water was added. The absorbance was measured at 228 nm. A blank group was prepared using the same procedures but without GSGH peptides. The restraining ability of GSGH peptides on ACE was defined as the difference in absorbance (%) between the sample group and the blank group at 228 nm. Moreover, the dose of GSGH peptides that was required to reduce ACE activity by 50% was defined as the IC<sub>50</sub> value.

In addition, the inhibition kinetics of GSGH peptides against ACE were analyzed with a Lineweaver–Burk plot.<sup>25</sup> Substrate (*N*-hippuryl-L-histidyl-L-leucine) concentration ranged from 0.13 to 1.32 mmol L<sup>-1</sup>, and the concentration of GSGH peptides used ranged from 0.008 to 0.042 mmol L<sup>-1</sup>. *K<sub>m</sub>* (Michaelis–Menten constant) and max velocity (*V<sub>m</sub>*) were both calculated from the Lineweaver–Burk plot.

### 2.6. Zinc-binding capacity

The 4-(2-pyridylazo)-resorcinol method was used to determine the zinc-binding capacity of GSGH peptides.<sup>26</sup> In the sample group, 1 mL of ZnCl<sub>2</sub> (0.5 mmol L<sup>-1</sup>), 1 mL of GSGH peptide solution (0.5 mg mL<sup>-1</sup>), 1 mL of 1,4-dithiothreitol (10 mmol L<sup>-1</sup>), and 7 mL of HEPES–KOH buffer (0.2 mmol L<sup>-1</sup>, pH 7.2) were added into a triangular glass bottle and mixed thoroughly. The bottle was shaken in the EZH-004C water bath oscillator (25 °C) at 225 rpm for 20 min. A blank control was prepared using the same procedure but without GSGH peptides. The zinc ion concentrations of the sample group and blank control were both determined and

recorded as *C<sub>s</sub>* and *C<sub>b</sub>*, respectively. The zinc-binding capacity of GSGH peptides (mg g<sup>-1</sup>) was defined as the reduction in zinc ion amount (mg) between the sample group and the blank group per the sample weight (g).

### 2.7. Identification and virtual screening of amino acid sequences

Peptide sequences of the GSGH subfraction possessing the strongest inhibiting power to ACE were analyzed with the same procedure and the same parameters described by Li *et al.*<sup>27</sup> Briefly, an AQCIYIY TDQ Quantum-Ultra mass spectrometer (Waters, Milford, Massachusetts, USA) coupled with electrospray ionization and Peak *de novo* 8.05 software (BSI, Waterloo, Ontario, Canada) was employed to conduct the quadrupole Orbitrap tandem spectrometric determination of GSGH peptides. The specific parameters for electrospray ionization operation were as follows: ion source gas of 60 psi; spray negative voltage of 4300 and positive voltage of 5300 V; mass range from 120 to 1600 *m/z*; and AGC target value of 1 × 10<sup>5</sup>. The threshold for an acceptable peptide sequence was 80%.<sup>7</sup> Validation of the GSGH amino acid sequences identified was carried out with the National Biotechnology Information Center (Bethesda, MD, USA) database. Afterward, the GSGH amino acid sequences obtained were virtually screened on the basis of a vector machine software score (SVMS) using the database AHTpin.<sup>28</sup> GSGH sequences that had a SVMS higher than zero were accepted as potential antihypertensive peptides.<sup>29</sup>

### 2.8. Chemosynthesis, physicochemical characteristics, and zinc binding power

The chemosynthesis of GSGH-derived sequences that were accepted as potential antihypertensive peptides was performed using the solid synthesis method at Yanqiao Peptide Synthesis Co. (Yancheng, China). The inhibiting capacity of the synthesized peptides on ACE and their binding power to zinc ions were both determined.<sup>25,26</sup> In addition, the physicochemical characteristics of GSGH peptides, especially hydrophilicity, hydrophobicity, and isoelectric point, were virtually analyzed using the database AHTpin.<sup>28</sup>

### 2.9. Virtual analysis of security

The toxicity of GSGH peptide sequences was analyzed using the database ToxinPred, while the potential allergenicity of GSGH peptide sequences was investigated by matching the allergenic sequences included in the database AlgPred.<sup>30</sup>

### 2.10. Molecular docking

Potential interaction models between GSGH peptides and ACE (PDB-108A) were virtually simulated by the software SYLLB 2.2.1 (SLERUXF-DCOK SRCEEN, Troesp Co., Missouri, USA) at the molecular level. The molecular spatial structure of ACE used in the current study was the PDB-108A structure. The evaluation index for the obtained interaction models contained total-score (*T*-score), Kuntz-D score, consistency score (*C*-score), Flex-Chem score, and Martin-PMF score. Of these, *T*-score was considered



the first evaluation index, and a molecular docking model should be accepted if its *T*-score is higher than 6.0.<sup>31</sup>

### 2.11. Chelation modes analysis with Fourier-transform infrared spectroscopy

In a stirring (135 rpm) glass triangular bottle, GSGH peptides (5 mg) were reacted with ZnCl<sub>2</sub> (100 μmol L<sup>-1</sup>, 25 mL) at 48 °C and pH 6.3 for the preparation of peptide–zinc chelate.<sup>27</sup> Twenty-five minutes later, the chelating solution was centrifuged at 4300 × *g* for 30 min. The supernatant was thoroughly mixed with four times the volume of anhydrous ethanol and then placed at 4 °C for 35 min to precipitate the GSGH peptide–zinc chelate. After centrifugation of the mixture at 12 300 × *g* for 20 min, the chelate (precipitate) was obtained, lyophilized, and stored at –20 °C.

Next, to investigate the chelation modes of GSGH peptides towards zinc ions, a FT-752 Fourier-transform infrared (FT-IR) spectrometer (Jinke Instrument Factory, Shanghai, China) was employed. Dried GSGH peptide–zinc chelate (3 mg) and 30 mg dried KBr were ground thoroughly in a mortar and then pressed into a translucent sheet.<sup>33</sup> The sheet was uploaded on an FT-752 FT-IR spectrometer and scanned at wavenumbers 4000–400 cm<sup>-1</sup>.

### 2.12. Stability analysis

As per the modified method of Sun *et al.*,<sup>33</sup> 50 mL of GSGH peptide solution (dissolved in deionized water, 3 mg mL<sup>-1</sup>) were added into a glass triangular bottle and adjusted to pH 2.00 ± 0.10 using HCl (0.1 mol L<sup>-1</sup>). The bottle was shaken at 165 rpm in the EZH-004C water bath oscillator (37 °C) for 5 min. Then, 5 mg of pepsin (10 U mg<sup>-1</sup>) was added to hydrolyze GSGH peptides. The digestion solution in the bottle was continuously shaken at 37 °C and 165 rpm in the oscillator. Ninety minutes later, the pH value of the digestion solution was adjusted to 7.00 ± 0.10 using NaOH (50 mmol L<sup>-1</sup>), and then 7.5 mg of trypsin (30 U mg<sup>-1</sup>) was added. The digestion solution was continuously shaken (165 rpm) at 37 °C for 2 h and then heated at 100 °C to inactivate the pepsin and trypsin. Eight minutes later, the digestion solution was cooled to room temperature, and the inhibiting capacity on ACE and binding power to zinc ions of GSGH peptides were both determined and compared with that of non-digested GSGH peptides.

### 2.13. Statistical analysis

All experiments were repeated three or more times. A statistical comparison between data was conducted on the Ver.15.0 SPSS program (SPSS Inc., Chicago, USA) using one-way analysis of variance tests and Duncan's multiple comparisons. The difference was considered significant at *P* < 0.05.

## 3. Results and discussion

### 3.1. Purification of GSGH fractions with high ACE-inhibitory activity

In the current study, the extraction rate of GSG was 22.65 ± 2.75 g × 100 g<sup>-1</sup>; and 41.65 ± 1.86 g of GSGH was prepared

from 100 g of GSG. It has been evidenced that Alcalase and thermolysin can both release peptide sequences containing aromatic amino acid Glu, Asp, or Arg residues from proteins.<sup>34</sup> These amino acid residues were instrumental in the capacity of peptides to inhibit ACE or bind with zinc ions.<sup>30,33</sup> Thus, Alcalase and thermolysin were used in sequence to hydrolyze ginkgo seed globulin. The hydrolysis degree of GSGH was 34.58% ± 4.79%, which was higher than that of *Ginkgo biloba* seed protein (27.22%).<sup>31</sup> Moreover, the zinc chelation ability and inhibitory effect against ACE of GSGH were 5.16 ± 0.17 mg g<sup>-1</sup> and 67.67% ± 3.33% (Fig. 1), respectively. Ma *et al.*<sup>22</sup> used Alcalase to hydrolyze ginkgo globulin, and the inhibitory ability of the hydrolysates against ACE was 43.89% ± 4.39%, which was lower than that of GSGH (*P* < 0.05).

As shown in Fig. 1A, four fractions, including GSGH-1, GSGH-2, GSGH-3, and GSGH-4, were isolated from GSGH after the gel chromatographic separation. Both the ACE-inhibitory activity (79.26% ± 6.39% at 1 mg mL<sup>-1</sup>) and zinc-chelating capacity (7.02 ± 0.22 mg g<sup>-1</sup>) of GSGH-4 were higher than those of other peaks (*P* < 0.05, Fig. 1B). After further purification on the S-D65 analytical chromatographic column, three peaks, separately named GSGH-4-A, GSGH-4-B, and GSGH-4-C, were presented on the RP-HPLC spectrum of GSGH-4 (Fig. 2A). The zinc chelation ratio of GSGH-4-C (11.39 ± 0.53 mg g<sup>-1</sup>) and its inhibition activity against ACE (85.74% ± 3.34%) were both higher than those of GSGH-4-A and GSGH-4-B (*P* < 0.05). These results demonstrated that peptide sequences possessing both zinc chelation ability and inhibition activity against ACE should be identified from GSGH-4-C.

### 3.2. Peptide sequences identification, virtual screening, and characterization

Previous studies have evidenced that ACE-inhibitory peptides are mainly oligopeptides containing fewer than 12 amino acid residues, and peptides with a molecular weight greater than 3000 Da are difficult to digest and absorb by the human body.<sup>8,25</sup> Table 1 shows that the oligopeptides containing fewer than 12 amino acid residues identified from GSGH-4-C: Ser-Pro-Pro-Thr-Ala-Ala-Ala (SPPTAAA), Ser-Ala-Thr-Ser-Ala-Ala-Ala-Ser-Met-Leu-Leu-Ser (SATSAAASMLLS), Asp-Gly-Ala-Val-Val-Gly-Gly-Pro-Asp-Gly-Arg (DGAHVGGPDGR), Pro-Ala-Ala-Ala-Ala-Ala-Ala-Gly-Ala-Gly (PAAAAAGAG), and Glu-Ala-Ser-Pro-Lys-Pro-Val (EASPKPV).

These sequences were virtually screened, and the results are shown in Table 1. The vector machine software score calculated by the database AHTpin is the main index to evaluate whether peptides have a potential antihypertensive effect.<sup>28</sup> Among these GSGH-4-A oligopeptides, only the vector machine software score of EASPKPV (0.89) was greater than the threshold value (0.00),<sup>28</sup> so it was accepted as an antihypertensive peptide. The ESI-MS/MS primary mass spectrum and secondary mass spectrum of EASPKPV are shown in Fig. 3A and B, respectively. Moreover, with increasing dose (*x*), the inhibiting power of EASPKPV on ACE (*y*) showed an exponential growth trend:  $y = 17.094 \ln(x) - 33.124$  (Fig. 4A), from which the IC<sub>50</sub> value of EASPKPV on inhibition capacity



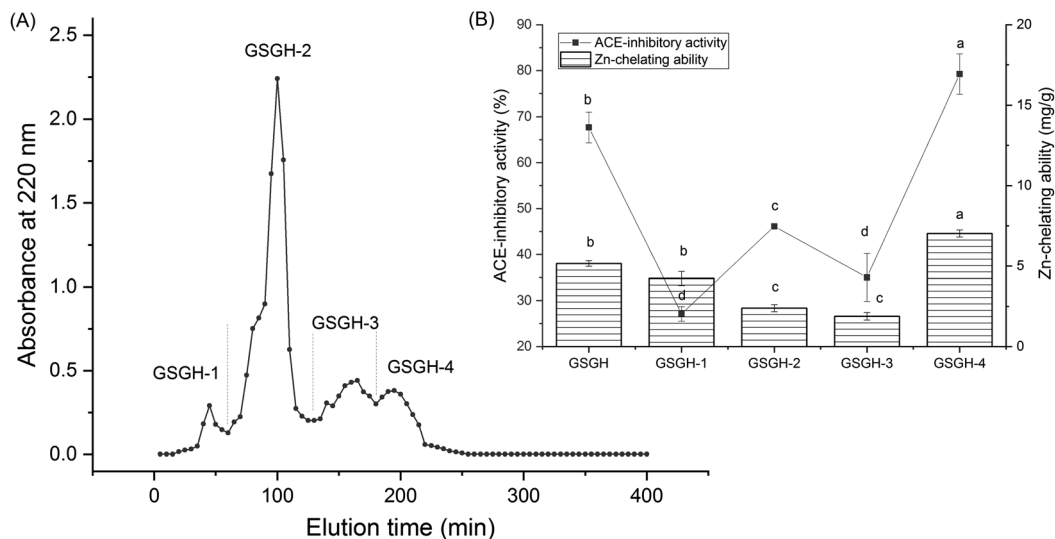


Fig. 1 (A) The chromatographic separation diagram of ginkgo seed globulin hydrolysates (GSGH) on Sephadex G-15 gel column, and (B) zinc ions chelating ability and inhibiting capacity against ACE of the separated main peaks separately named as GSGH-1, GSGH-2, GSGH-3 and GSGH-4. Different letters (a–d) between the groups marked a statistically significant difference ( $P < 0.05$ ).

against ACE was calculated to be  $87.66 \pm 2.96 \mu\text{mol L}^{-1}$ . This value was lower than that of peptides YSCPFR identified from camel milk ( $\text{IC}_{50}$ :  $312 \mu\text{mol L}^{-1}$ ) and FMRWRD isolated from Tombul hazelnut ( $\text{IC}_{50}$ :  $259.7 \mu\text{mol L}^{-1}$ ),<sup>24,34</sup> but was higher than that of captopril, which was a widely used antihypertensive drug with a  $\text{IC}_{50}$  of  $0.14 \mu\text{mol L}^{-1}$ .<sup>12</sup> Since the  $\text{IC}_{50}$  value was inversely proportional to the inhibiting power of peptides on ACE, EASPKPV showed a better inhibiting effect on ACE than YSCPFR and FMRWRD, but its inhibiting ability was poorer than that of captopril.

Numerous studies have demonstrated that the amino acid composition of peptides, especially C-terminal tripeptides, is instrumental in their inhibiting power on ACE. Hydrophobic amino acid residues in the C-terminal, especially aromatic amino acids and branched amino acids (Val, Ile, and Leu), were shown to have strong binding power to the active binding sites of ACE.<sup>35</sup> EASPKPV contained Pro and Val residues in the C-terminal, which were both hydrophobic, so it offered a relatively high ACE-inhibitory activity ( $87.66 \mu\text{mol L}^{-1}$ ). Moreover, Lys residue in C-terminal tripeptides of peptides has been

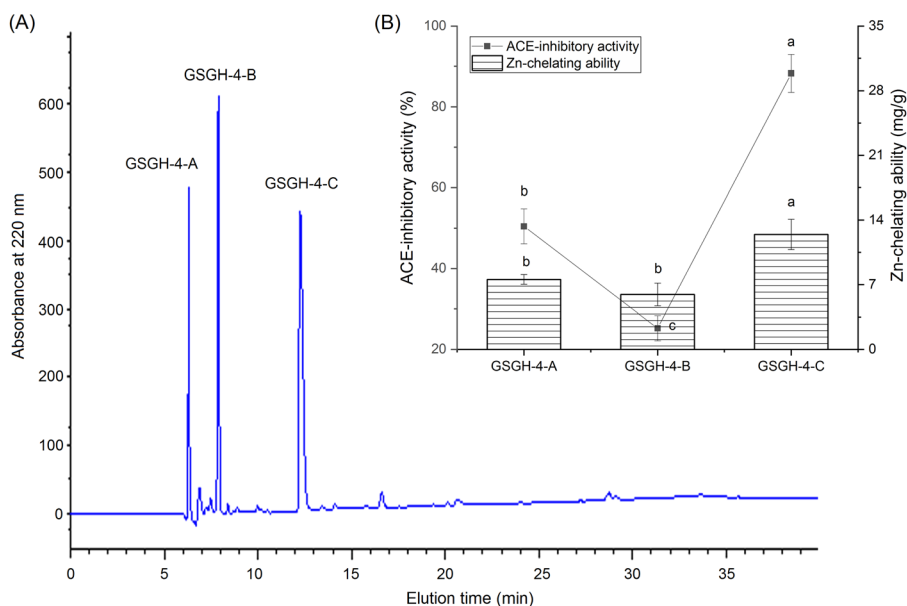


Fig. 2 (A) The chromatographic separation diagram of GSGH-4 in reverse-phase high performance liquid chromatography system, and (B) the zinc ions chelating ability and inhibiting capacity against ACE of the separated main peaks named as GSGH-4-A, GSGH-4-B and GSGH-4-C. Different letters (a–c) between the groups marked a statistically significant difference ( $P < 0.05$ ).



**Table 1** *In silico* screening, chelating ability towards zinc ions, inhibitory effect against ACE, and stability of sequences from ginkgo seed globulin hydrolysates

Peptide sequence	EASPKPV	DGAVVGGPDGR	SATSAAASMLLS	SPPTAAA	PAAAAAAGAG
Mass (Da)	726.91	999.2	1109.39	613.74	726.9
Matched sequence in <i>Ginkgo biloba</i> <sup>a</sup>	P.EEASPKPV.I	L.DGAVVGGPDGR.D	A.SATSAAASMLLS.G	F.SPPTAAA.A	P.PAAAAAAGAG.A
Vector machine software score <sup>b</sup>	0.94	-1.21	-0.95	-1.5	-0.31
Antihypertension prediction <sup>c</sup>	AHP	Non-AHP	Non-AHP	Non-AHP	Non-AHP
Inhibitory effect against ACE (IC <sub>50</sub> : μmol L <sup>-1</sup> )	87.66 ± 2.96	ND	ND	ND	ND
Inhibitory effect against ACE after gastrointestinal digestion (IC <sub>50</sub> : μmol L <sup>-1</sup> )	93.56 ± 7.38	ND	ND	ND	ND
Chelating ability towards zinc ions (mg g <sup>-1</sup> )	5.35 ± 0.32e	14.99 ± 0.35d	0.07 ± 0.01f	0.22 ± 0.01f	0.42 ± 0.03f
Chelating ability towards zinc ions after gastrointestinal digestion (mg g <sup>-1</sup> )	5.77 ± 0.37	ND	ND	ND	ND

<sup>a</sup> From National Center for Biotechnology Information (NCBI). <sup>b</sup> Vector machine software score and potential antihypertension were *in silico* screened with database AHTPIN. <sup>c</sup> AHP: antihypertensive peptide. ND: not measured. Different letters (d-f) between the groups marked a statistically significant difference ( $P < 0.05$ ).

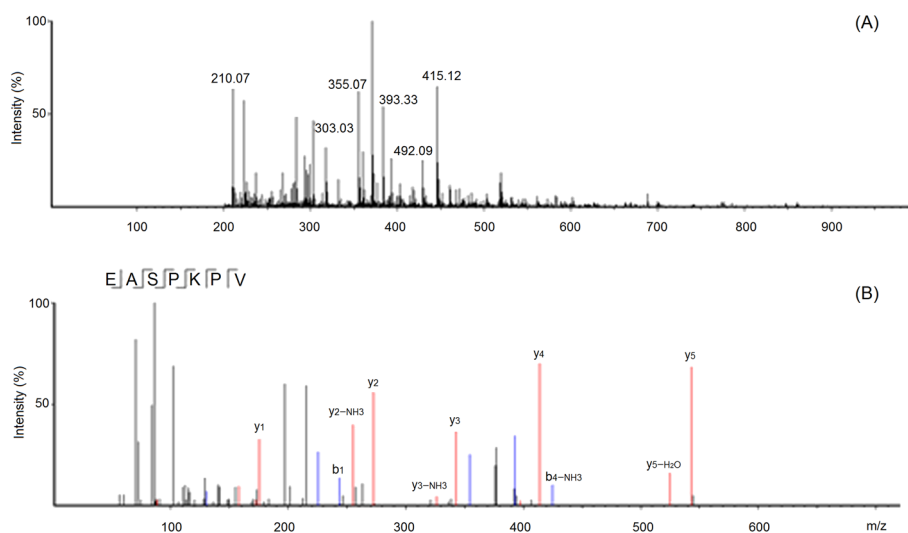
evidenced to increase the inhibiting effect of peptides on ACE.<sup>25,36</sup> Peptides with Lys residue in C-terminal tripeptides such as PPKP and PKPP derived from walnut protein,<sup>37</sup> and WNGPKGV from corn protein,<sup>11</sup> all exhibited excellent inhibiting ability on ACE.

### 3.3. Zinc-binding ability and physicochemical parameters

The chelating abilities of EASPKPV and DGAVVGGPDGR towards zinc ions were 5.35 and 14.99 mg g<sup>-1</sup>, respectively (Table 1), which were higher than that of TGLL from coconut cake globulin (2.27 mg g<sup>-1</sup>), but lower than that of ethylenediamine tetraacetic acid (57.17 mg g<sup>-1</sup>).<sup>32,38</sup> The high content of Asp (18.18%, Table 2) was mainly responsible for the high chelating ability of DGAVVGGPDGR towards zinc ions because the γ-carboxyl group of Asp can significantly increase the negative polarity of peptides, which is the main binding force between peptides and zinc ions.<sup>39</sup> In the case of EASPKPV, the γ-carboxyl group of Glu and the ε-amino group of Lys, which were both effective sites for the chelation of zinc

ions, mainly contributed to the zinc binding power of EASPKPV.<sup>30</sup> Furthermore, both EASPKPV and DGAVVGGPDGR had high hydrophilicity (0.61 and 0.50, respectively, Table 2), which was one of the main reasons for their high zinc-binding power, for hydrophilicity reflected the polarity of polypeptide that was positively correlated with their binding affinity with zinc ions.<sup>33</sup> There is zinc tetrahedral coordination in ACE. This zinc coordination plays an important role in the catalyzing effect of ACE.<sup>8</sup> Previous studies showed that peptides with strong zinc chelating ability probably offered high inhibition capacity against ACE.<sup>5,38</sup> Thus, the relatively high zinc chelating ability of EASPKPV may be one reason for its high ACE-inhibitory activity.

The isoelectric points (pI) of EASPKPV and DGAVVGGPDGR were 6.35 and 4.21, respectively (Table 2), suggesting that EASPKPV, DGAVVGGPDGR, and their zinc chelation should avoid being used in these pH values. The reason was that the surface net charge of peptides was nearly zero and their polarity

**Fig. 3** The primary mass spectrum (A) and secondary mass spectrum (B) of peptides EASPKPV with UPLC-Q-TOF-MS/MS.

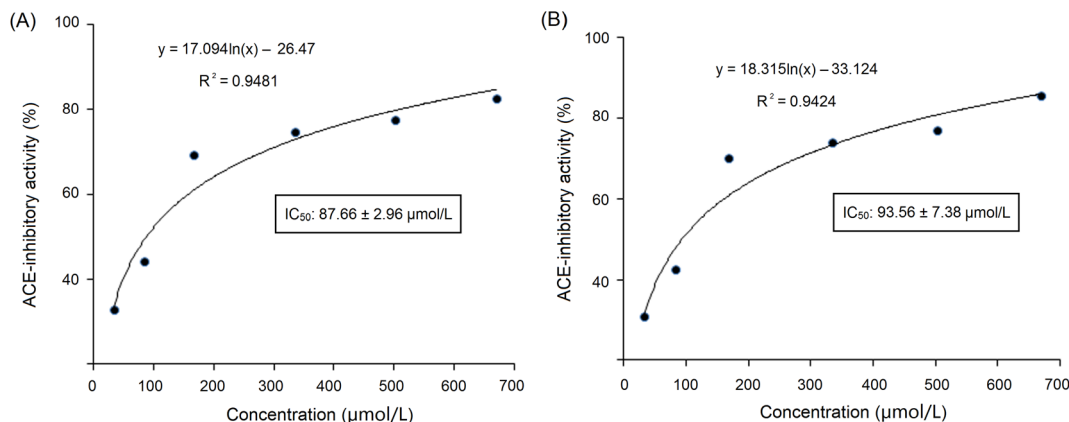


Fig. 4 (A) The inhibitory effect of EASPKPV on ACE against different dose, and the fitting equation; and (B) the ACE inhibitory effect of EASPKPV digested by gastrointestinal enzymes, and the fitting equation.

was low at pI, resulting in a low capacity of peptides to inhibit ACE or chelate with zinc ions at pI.<sup>31</sup> Zheng *et al.* found coconut peptide showed lower zinc-chelation ability at pI (pH 3.58).<sup>38</sup>

### 3.4. Safety analysis

Potential toxicity and allergenicity will prevent the use of health-care peptides in foods. It has been stated that eating more than six *Ginkgo biloba* seeds could cause human poisoning.<sup>16</sup> Thus, analysis of the safety of ginkgo seed globulin peptides is necessary. The *in silico* analytical results on the toxicity and potential allergenicity of GSGH-4-A peptides are shown in Table 2. It was shown that GSGH-4-A peptides, including EASPKPV, DGAVVGGPDGR, SATSAAASMLLS, SPPTAAA, and PAAAAAAGAG, obtained in this study were all non-toxic and non-allergenic. However, these data are only the results of *in silico* prediction. The safety of these GSGH-4-A peptides still needs to be verified *in vitro* and *in vivo*.

### 3.5. ACE-restrain mechanism analysis

**3.5.1 Docking modes between EASPKPV and ACE.** Fig. 5a shows the local diagram of the best docking mode for EASPKPV towards ACE (with a high *T*-score of 8.4), while Fig. 5b depicts the global diagram. The results in Fig. 5a and Table 3 evidence

that EASPKPV can interact with multiple sites of ACE *via* hydrogen bonds or hydrophobic interactions. Among these sites, any one of Gln281, His353, Ala354, Glu376, Lys511, and Tyr523 can be linked with EASPKPV by short hydrogen bonds. Tyr523 and Ala354 are the central residues of the S1 central pocket in ACE, while His353, Gln281, and Lys511 are located in the S2 central pocket of ACE. Both the S1 pocket and the S2 pocket belong to the active center of ACE.<sup>4</sup> Moreover, of the thirteen active residues that interacted with EASPKPV through hydrophobic interactions (Table 3), His383 is one residue of zinc tetrahedral coordination that is located in the catalytic center of ACE.<sup>25</sup> Additionally, the results in Table 1 show that EASPKPV had a high affinity for zinc ions. Thus, EASPKPV can inhibit ACE *via* binding with the S1 pocket, S2 pocket, and/or zinc tetrahedral coordination, indicating that EASPKPV was a competitive inhibitor of ACE, which was consistent with the inhibition kinetics results as shown in Fig. 6. An increasing number of studies have shown that the inhibitory effect of competitive inhibitors on ACE is strong.<sup>6,8,40</sup> In the current study, the *T*-score and *C*-score for the optimal docking mode between ACE and EASPKPV were 8.42 and 5.0, respectively, both higher than the accepted threshold.<sup>25</sup> In addition, the hydrogen bond distance between EASPKPV and the five central active sites (Gln281, Ala354, Glu376, Lys511, and Tyr523) was short (2.69–

Table 2 *In silico* analysis of the physicochemical characteristics of ginkgo seed globulin peptides using the AHTpin database

Peptides	EASPKPV	DGAVVGGPDGR	SATSAAASMLLS	SPPTAAA	PAAAAAAGAG
Acidic and basic amino acid content (%)	28.57%	27.27%	0.00%	0.00%	0.00%
Hydrophobic amino acid content (%)	57.14%	36.36%	58.33%	71.43%	80.00%
Hydrophobicity	−0.19	−0.12	0.09	0.02	0.20
Amphiphilicity	0.71	0.22	0.00	0.00	0.00
Hydrophilicity	0.61	0.50	−0.51	−0.23	−0.35
Net hydrogen	0.57	0.55	0.42	0.29	0.00
Solvation	0.46	0.03	0.79	0.71	0.59
Charge	0	−1	0	0	0
Isoelectric point	6.35	4.21	5.88	5.88	5.88
Toxicity	Non-toxic	Non-toxic	Non-toxic	Non-toxic	Non-toxic
Allergenicity	Non-allergenic	Non-allergenic	Non-allergenic	Non-allergenic	Non-allergenic



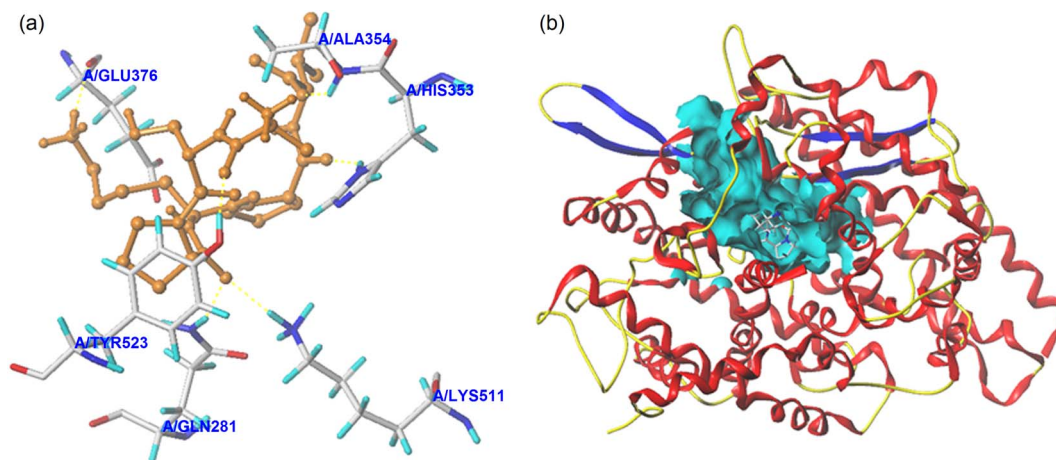


Fig. 5 The local diagram (a) and global diagram (b) of the best docking patterns between EASPKPV and ACE. The structure of ACE was used PDB 1O8A model.

3.05 Å), suggesting that EASPKPV had a strong affinity towards ACE. Therefore, the interacting mode and strong binding affinity were the main reasons for the high inhibitory effect of EASPKPV on ACE ( $IC_{50}$ :  $87.66 \pm 2.96 \mu\text{mol L}^{-1}$ ; Fig. 4A).

**3.5.2 Restrain kinetics of ACE.** Fig. 6 shows the inhibiting effect of EASPKPV with different doses (0.014–0.069  $\text{mmol L}^{-1}$ ) on ACE kinetics. The Lineweaver–Burk diagram showed that the maximum velocity ( $V_{\text{max}}$ ) was constant, but the  $K_m$  increased with increasing EASPKPV dose, which was the typical efficacy of competitive inhibitors on ACE.<sup>7</sup> So, EASPKPV was a competitive inhibitor for ACE, which was consistent with the results as shown in Fig. 5 and Table 3. Peptide YIRLHF identified from bighead carp protein also showed competitive inhibitory kinetics and offered high restraining ability on ACE ( $IC_{50}$ :  $121.90 \mu\text{mol L}^{-1}$ ).<sup>41</sup>

**3.5.3 The binding mode of EASPKPV to zinc ion.** Zinc tetrahedral coordination, consisting of a zinc ion attached to three residues (His383, His387, and Glu411), plays an important role in the catalytic function of ACE.<sup>5</sup> In the current study, to further study the effect of EASPKPV on the zinc tetrahedral coordination of ACE, especially the zinc ions, Fourier-transform infrared spectroscopy was employed, and the results are shown in Fig. 7. In general, EASPKPV–zinc chelate and pure EASPKPV

showed similar FT-IR spectra, but there were obvious differences between them. In the FT-IR spectrum of EASPKPV, the peaks located at 3360, 1660, and 815  $\text{cm}^{-1}$  separately

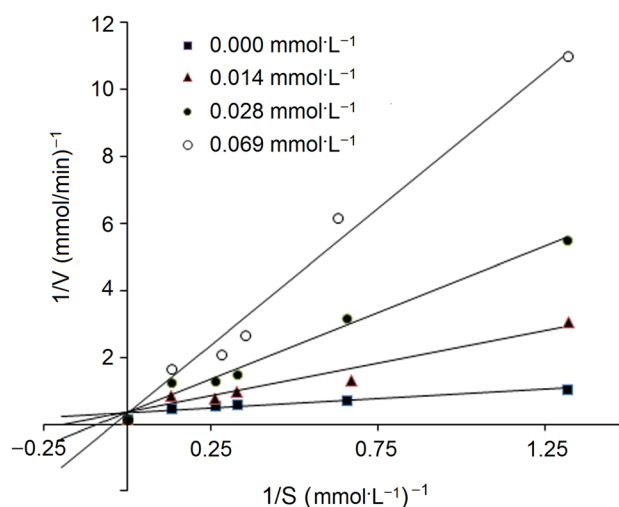


Fig. 6 Lineweaver–Burk chart for inhibitory capacity of EASPKPV towards ACE.

Table 3 Virtual evaluation of the docking modes of EASPKPV with ACE and interaction forces in the best mode<sup>a</sup>

Ligand	T-Score	C-Score	Interaction force	Active sites of ACE and hydrogen bond length
EASPKPV	8.42	5	Hydrogen bond	Gln281 (2.72 Å); His353 (2.71 Å); Ala354 (2.69 Å); Glu376 (2.93 Å); Lys511 (3.05 Å); Tyr523 (2.84 Å)
			Hydrophobic interactions	Glu162; Gln369; Asp377; Ser355; His383; Tyr520; Phe457; Val380; Val379; Trp279; Asn277; Thr166; Cys370

<sup>a</sup> T-Score is the total score of the virtual evaluation, and C-score is the consistency score.





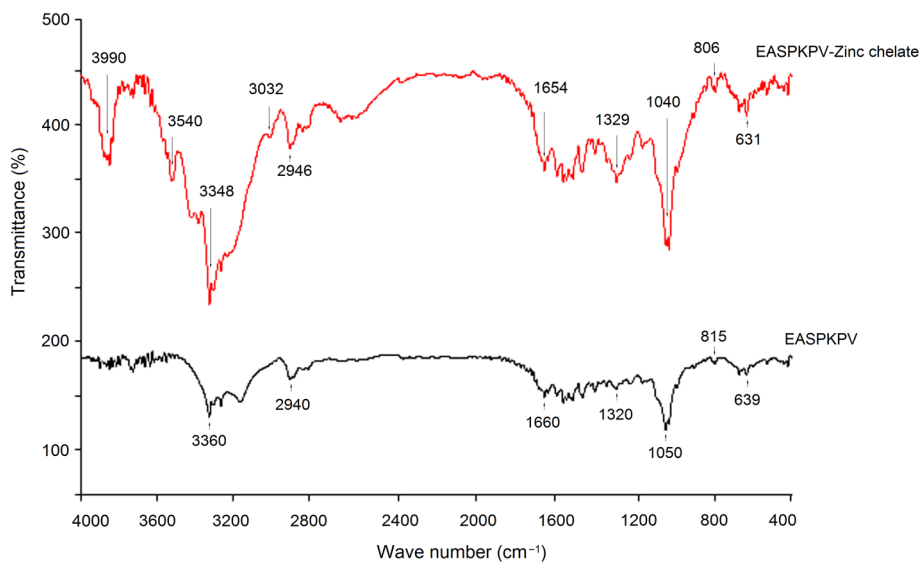


Fig. 7 Fourier-transformed infrared spectroscopic diagrams of EASPKPV–zinc ligands. Pure EASPKPV was used as comparison.

represented the stretching of  $-N-H$ ,  $-C-N$ , and amide IV bands.<sup>32,39</sup> These peaks transferred to 3348, 1654, and 806  $\text{cm}^{-1}$  after zinc chelation, respectively, demonstrating that both peptide bonds and the amino group of EASPKPV linked with zinc ions.<sup>27</sup> Furthermore, the carboxyl group of EASPKPV also chelated with zinc ions, because peaks at 1320 and 1050  $\text{cm}^{-1}$ , both corresponding to the asymmetric bend of  $-C-O$ ,<sup>33</sup> shifted to 1329 and 1040  $\text{cm}^{-1}$ , respectively. These results highlighted the potency with which EASPKPV can interact with the zinc tetrahedral coordination of ACE *via* binding to the zinc ion. Although previous studies showed that peptides with high zinc chelating ability always had a high capacity to inhibit ACE, Zheng *et al.* demonstrated that the addition of zinc ions reduced the ACE-inhibitory activity of camellia peptides.<sup>42</sup> Thus, the binding pattern of EASPKPV, the zinc tetrahedral coordination, and the effect of zinc chelation on its ACE-inhibitory activity require further investigation.

### 3.6. Stability against gastrointestinal digestion

As dose ( $x$ ) increased, the ACE-inhibiting power of EASPKPV digested by pepsin and trypsin ( $y$ ) exhibited an exponential growth trend:  $y = 18.315 \ln(x) - 33.124$  (Fig. 4B), from which the ACE-inhibition  $IC_{50}$  value of EASPKPV digested by pepsin and trypsin was calculated to be  $93.56 \pm 7.38 \mu\text{mol L}^{-1}$ . This value was similar to that of the untreated EASPKPV ( $87.66 \pm 2.96 \mu\text{mol L}^{-1}$ , Fig. 4A) ( $P > 0.05$ ). In addition, the zinc-binding affinity of EASPKPV digested by pepsin and trypsin was  $5.77 \pm 0.37 \text{ mg g}^{-1}$  (Table 2), which was nearly equal to that of EASPKPV ( $5.35 \pm 0.32 \text{ mg g}^{-1}$ ) ( $P > 0.5$ ). These results evidenced that the hydrolysis of pepsin and trypsin had no remarkable efficacy on the abilities of EASPKPV to inhibit ACE and bind to zinc ions ( $P > 0.5$ ). The reason perhaps was that EASPKPV contained a high content of the Pro residue. The rigid ring structure in Pro was shown to improve the stability of peptides under gastrointestinal digestion.<sup>10,39</sup> Oligopeptides

such as LSMSFPPF, VPKIPPP, and PPSEPTKL (derived from ginkgo seed and bighead carp), containing a high content of Pro, also exhibited excellent stability against gastrointestinal enzymic digestion.<sup>21,41</sup> However, the effect of gastrointestinal enzymes on the structure of EASPKPV should be investigated in future studies.

## 4. Conclusions

Five oligopeptides containing less than 12 amino acid residues were isolated from GSGH in this study. Of these oligopeptides, EASPKPV showed relatively high capacities to restrain ACE ( $IC_{50}$ :  $87.66 \mu\text{mol L}^{-1}$ ) and bind with zinc ions ( $5.35 \pm 0.32 \text{ mg g}^{-1}$ ). The mechanisms of EASPKPV to restrain ACE probably contain the following ways: (i) competitively linking with five key active residues (Gln281, Ala354, Glu376, Lys511, and Tyr523) in the S1 pocket and S2 pocket of ACE by short hydrogen bonds; (ii) binding to thirteen active residues of ACE *via* hydrophobic interactions; and (iii) binding with residue His383 or the zinc ion of the zinc tetrahedral coordination in ACE. Moreover, the digestion of trypsin and pepsin did not show any remarkable efficacy on the capacities of EASPKPV to restrain ACE and bind with zinc ions. However, the *in vivo* antihypertensive effect of EASPKPV requires further work.

## Author contributions

Wei Gao: investigation, methodology, writing—original draft. Min Liu: conceptualization, validation, writing—review, funding acquisition. Yu Wang: writing—review, funding acquisition.

## Conflicts of interest

There are no conflicts to declare.



## Acknowledgements

This work was supported by the Natural Science Foundation of Shanxi Province, China (202203021221139).

## References

- W. Xue, W. Zhao, S. Wu and Z. Yu, Underlying anti-hypertensive mechanism of the Mizuhopecten yessoensis derived peptide NCW in spontaneously hypertensive rats via widely targeted kidney metabolomics, *Food Sci. Hum. Wellness*, 2024, **13**, 472–481.
- J. Wu, W. Liao and C. C. Udenigwe, Revisiting the mechanisms of ACE inhibitory peptides from food proteins, *Trends Food Sci. Technol.*, 2017, **69**, 214–219.
- X. Duan, Y. Dong, M. Zhang, Z. Li, G. Bu and F. Chen, Identification and molecular interactions of novel ACE inhibitory peptides from rapeseed protein, *Food Chem.*, 2023, **422**, 136085.
- Z. Li, Y. He, H. He, W. Zhou, M. Li, A. Lu, T. Che and S. Shen, Purification identification and function analysis of ACE inhibitory peptide from *Ulva prolifera* protein, *Food Chem.*, 2023, **345**, 134127.
- A. Pina and A. Roque, Studies on the molecular recognition between bioactive peptides and angiotensin-converting enzyme, *J. Mol. Recognit.*, 2009, **22**, 162–168.
- R. Li., X. Zhou, L. Sun and Y. Zhuang, Identification, in silico screening, and molecular docking of novel ACE inhibitory peptides isolated from the edible symbiot *Boletus griseus*-*Hypomyces chrysospermus*, *LWT-Food Sci. Technol.*, 2022, **169**, 114008.
- S. Y. Ruan, L. P. Sun, X. D. Sun, J. L. He and Y. L. Zhuang, Novel umami peptides from tilapia lower jaw and molecular docking to the taste receptor T1R1/T1R3, *Food Chem.*, 2021, **362**(15), 130249.
- S. Y. Lee and S. J. Hur, Antihypertensive peptides from animal products, marine organisms, and plants, *Food Chem.*, 2017, **228**, 506–517.
- N. P. Nirmal, M. S. Rajput, N. B. Rathod, P. Mudgil, S. Pati, G. Bono, S. Nalinanon, L. Li and S. Maqsood, Structural characteristic and molecular docking simulation of fish protein-derived peptides: recent updates on antioxidant, anti-hypertensive and anti-diabetic peptides, *Food Chem.*, 2023, **405**, 134737.
- B. P. Singh and S. Vij, In vitro stability of bioactive peptides derived from fermented soy milk against heat treatment, pH and gastrointestinal enzymes, *LWT-Food Sci. Technol.*, 2018, **91**, 303–307.
- W. Wongngam, A. Hamzeh, F. Tian, S. Roytrakul and J. Yongsawatdigul, Purification and molecular docking of angiotensin converting enzyme-inhibitory peptides derived from corn gluten meal hydrolysate and from in silico gastrointestinal digestion, *Process Biochem.*, 2023, **129**(38), 113–120.
- O. Magouz, N. Mehanna, M. Khalifa, H. Sakr, S. Gensberger-Reigl, S. Dalabasmaz and M. Pischetsrieder, Profiles, antioxidative and ACE inhibitory activity of peptides released from fermented buttermilk before and after simulated gastrointestinal digestion, *Innovative Food Sci. Emerging Technol.*, 2023, **84**, 103266.
- Z. Zou, M. Wang, Z. Wang, R. E. Aluko and R. He, Antihypertensive and antioxidant activities of enzymatic wheat bran protein hydrolysates, *J. Food Biochem.*, 2020, **44**(1), e13090.
- I. D. Boateng and X. Yang, Ginkgo biloba L. seed; a comprehensive review of bioactives, toxicants, and processing effects, *Ind. Crop. Prod.*, 2022, **176**, 114281.
- S. F. Omidkhoda, B. B. M. Razavi and H. Hosseinzadeh, Protective effects of Ginkgo biloba L. against natural toxins, chemical toxicities, and radiation: a comprehensive review, *Phytother. Res.*, 2019, **33**(11), 2821–2840.
- H. Y. Wang and Y. Q. Zhang, The main active constituents and detoxification process of Ginkgo biloba seeds and their potential use in functional health foods, *J. Food Compos. Anal.*, 2019, **83**, 103247.
- I. D. Boateng, X. M. Yang and Y. Y. Li, Optimization of infrared-drying parameters for Ginkgo biloba L. seed and evaluation of product quality and bioactivity, *Ind. Crop. Prod.*, 2020, **160**, 113108.
- X.-G. Liu, X. Lu, W. Gao, P. Li and H. Yang, Structure, synthesis, biosynthesis, and activity of the characteristic compounds from Ginkgo biloba L., *Nat. Prod. Rep.*, 2022, **39**(3), 474–511.
- Q. Deng, L. Wang, F. Wei, B. Xie, F. Huang, W. Huang, J. Shi, Q. Huang, B. Tian and S. Xue, Functional properties of protein isolates, globulin and albumin extracted from Ginkgo biloba seeds, *Food Chem.*, 2011, **124**(4), 1458–1465.
- W. Zhang, C. Liu, J. Zhao, T. Ma, Z. He, M. Huang and Y. Wang, Modification of structure and functionalities of ginkgo seed proteins by pH-shifting treatment, *Food Chem.*, 2021, **358**, 129862.
- X. Wang, Y. Deng, P. Xie, L. Liu, C. Zhang, J. Cheng, Y. Zhang, Y. Liu, L. Huang and J. Jiang, Novel bioactive peptides from ginkgo biloba seed protein and evaluation of their  $\alpha$ -glucosidase inhibition activity, *Food Chem.*, 2023, **404**, 134481.
- F.-F. Ma, H. Wang, C.-K. Wei, K. Thakur, Z.-J. Wei and L. Jiang, Three novel ACE inhibitory peptides isolated from Ginkgo biloba seeds: purification, inhibitory kinetic and mechanism, *Front. Pharmacol.*, 2019, **9**, 1579.
- P. M. Nielsen, D. Petersen and C. Dambmann, Improved method for determining food protein degree of hydrolysis, *J. Food Sci.*, 2001, **66**(5), 642–646.
- R. Khakhariya, B. Basaiawmoit, A. A. Sakure, R. Maurya, M. Bishnoi, K. K. Kondepudi, S. Padhi, A. K. Rai, Z. Liu and S. Hati, Production and Characterization of ACE Inhibitory and Anti-Diabetic Peptides from Buffalo and Camel Milk Fermented with *Lactobacillus* and Yeast: A Comparative Analysis with In Vitro, In Silico, and Molecular Interaction Study, *Foods*, 2023, **12**, 2006.
- U. Urbizo-Reyes, A. M. Liceaga, L. Reddivari, K.-H. Kim and J. M. Anderson, Enzyme kinetics, molecular docking, and in silico characterization of canary seed (Phalaris



- canariensis L.) peptides with ACE and pancreatic lipase inhibitory activity, *J. Funct. Foods*, 2022, **88**, 104892.
- 26 X. Ke, X. Hu, L. Li, X. Yang, S. Chen, Y. Wu and C. Xue, A novel zinc-binding peptide identified from tilapia (*Oreochromis niloticus*) skin collagen and transport pathway across Caco-2 monolayers, *Food Biosci.*, 2022, **42**, 101127.
- 27 Y. Li, P. Shi, Y. Zheng, M. Guo, Y. Zhuang and X. Huo, Millet bran protein hydrolysates derived peptides-zinc chelate: structural characterization, security prediction in silico, zinc transport capacity and stability against different food processing conditions, *J. Food Sci.*, 2023, **88**, 477–490.
- 28 R. Kumar, K. Chaudhary, M. Sharma, G. Nagpal, J. S. Chauhan, S. Singh, A. Gautam and G. P. Raghava, AHTPDB: a comprehensive platform for analysis and presentation of antihypertensive peptides, *Nucleic Acids Res.*, 2015, **43**, D956–D962.
- 29 N. D. Zaharuddin, I. Barkia, W. Z. W. Ibadullah, M. Zarei and N. Saari, Identification, molecular docking, and kinetic studies of six novel angiotensin-I-converting enzyme (ACE) inhibitory peptides derived from Kenaf (*Hibiscus cannabinus* L.) seed, *Int. J. Biol. Macromol.*, 2022, **220**, 1512–1522.
- 30 S. Gupta, P. Kapoor, K. Chaudhary, A. Gautam, R. Kumar and G. P. S. Raghava, Open Source Drug Discovery Consortium. In Silico Approach for Predicting Toxicity of Peptides and Proteins, *PLoS One*, 2013, **8**, e73957.
- 31 M. Zarei, R. Ghanbari, N. Zainal, R. Ovissipour and N. Saari, Inhibition kinetics, molecular docking, and stability studies of the effect of papain-generated peptides from palm kernel cake proteins on angiotensin-converting enzyme (ACE), *Food Chem.: Mol. Sci.*, 2022, **5**, 100147.
- 32 Z. Zhang, F. Zhou, X. Liu and M. Zhao, Particulate nanocomposite from oyster (*Crassostrea rivularis*) hydrolysates via zinc chelation improves zinc solubility and peptide activity, *Food Chem.*, 2018, **258**, 269–277.
- 33 R. Sun, X. Liu, Y. Yu, J. Miao, K. Leng and H. Gao, Preparation process optimization, structural characterization and in vitro digestion stability analysis of Antarctic krill (*Euphausia superba*) peptides-zinc chelate, *Food Chem.*, 2021, **340**, 128056.
- 34 A. F. Çâğlar, A. G. Göksu, B. Çakır and I. Gülseren, Tombul hazelnut (*Corylus avellana* L.) peptides with DPP-IV inhibitory activity: in vitro and in silico studies, *Food Chem.: X*, 2021, **12**, 100151.
- 35 O. Abdelhedi, R. Nasri, M. Jridi, L. Mora, E. Oseguera-Toledo, M. Aristoy, B. Amara, F. Toldrá and M. Nasri, In silico analysis and antihypertensive effect of ACE-inhibitory peptides from smooth-hound viscera protein hydrolysate: enzyme-peptide interaction study using molecular docking simulation, *Process Biochem.*, 2017, **58**, 145–159.
- 36 M. M. Abedin, R. Chourasia, L. C. Phukon, S. P. Singh and A. K. Rai, Characterization of ACE inhibitory and antioxidant peptides in yak and cow milk hard chhurpi cheese of the Sikkim Himalayan region, *Food Chem.: X*, 2022, **13**, 100231.
- 37 H. Tang, C. Wang, S. Cao and F. Wang, Novel angiotensin I-converting enzyme (ACE) inhibitory peptides from walnut protein isolate: separation, identification and molecular docking study, *J. Food Biochem.*, 2022, **46**(12), e14411, DOI: [10.1111/jfbc.14411](https://doi.org/10.1111/jfbc.14411).
- 38 Y. Zheng, M. Guo, C. Cheng, J. Li, Y. Li, Z. Hou and Y. Ai, Structural and physicochemical characteristics, stability, toxicity and antioxidant activity of peptide-zinc chelate from coconut cake globulin hydrolysates, *LWT–Food Sci. Technol.*, 2023, **173**, 114367.
- 39 M. C. Udechukwu, B. Downey and C. C. Udenigwe, Influence of structural and surface properties of whey-derived peptides on zinc-chelating capacity, and in vitro gastric stability and bioaccessibility of the zinc-peptide complexes, *Food Chem.*, 2018, **240**, 1227–1232.
- 40 H. Shukla, A. Sakure, R. Maurya, M. Bishnoi, K. K. Kondepudi, S. Das, Z. Liu, S. Padhi, A. K. Rai and S. Hati, Antidiabetic, angiotensin-converting enzyme inhibitory and anti-inflammatory activities of fermented camel milk and characterisation of novel bioactive peptides from lactic-fermented camel milk with molecular interaction study, *Int. J. Dairy Technol.*, 2023, **76**(1), 149–167.
- 41 M. Chen, L. Wang, C. Zheng, A. Ma, K. Hu, A. Xiang, Z. Sun, B. Xie, G. Xiong, L. Shi, S. Chen and W. Wu, Novel ACE inhibitory peptides derived from bighead carp (*Aristichthys nobilis*) hydrolysates: screening, inhibition mechanisms and the bioconjugation effect with graphene oxide, *Food Biosci.*, 2023, **52**, 102399.
- 42 Y. J. Zheng, P. Q. Shi, Y. Li, Y. L. Zhuang, Y. L. Zhang, L. Liu and W. Wang, A novel ACE-inhibitory hexapeptide from camellia glutelin-2 hydrolysates: identification, characterization and stability profiles under different food processing conditions, *LWT–Food Sci. Technol.*, 2021, **147**, 111682.

